AIP | Applied Physics Letters

Hole electrical transporting properties in organic-Si Schottky solar cell

Xiaojuan Shen, Yawen Zhu, Tao Song, Shuit-Tong Lee, and Baoquan Sun

Citation: Appl. Phys. Lett. **103**, 013504 (2013); doi: 10.1063/1.4812988
View online: http://dx.doi.org/10.1063/1.4812988
View Table of Contents: http://apl.aip.org/resource/1/APPLAB/v103/i1
Published by the AIP Publishing LLC.

Additional information on Appl. Phys. Lett.

Journal Homepage: http://apl.aip.org/
Journal Information: http://apl.aip.org/about/about_the_journal
Top downloads: http://apl.aip.org/features/most_downloaded
Information for Authors: http://apl.aip.org/authors

ADVERTISEMENT

Downloaded 17 Sep 2013 to 147.26.11.80. This article is copyrighted as indicated in the abstract. Reuse of AIP content is subject to the terms at: http://apl.aip.org/about/rights_and_permissions

Hole electrical transporting properties in organic-Si Schottky solar cell

Xiaojuan Shen, Yawen Zhu, Tao Song, Shuit-Tong Lee, and Baoquan Sun[a)]
Jiangsu Key Laboratory for Carbon-Based Functional Materials & Devices, Institute of Functional Nano & Soft Materials (FUNSOM), Soochow University, 199 Ren'ai Road, Suzhou 215123, China

(Received 13 May 2013; accepted 16 June 2013; published online 2 July 2013)

In this work we investigated the hole electrical transporting properties effect on the organic-Si hybrid Schottky solar cells. By changing the post-annealing atmosphere of poly(3,4-ethylenedioxythiophene)/poly(styrenesulfonate) (PEDOT:PSS) film, the power conversion efficiencies of the Schottky Si/PEDOT:PSS cell boosted from 6.40% in air to 9.33% in nitrogen. Current-voltage, capacitance-voltage, external quantum efficiency, and transient photovoltage measurements illustrated that the enhanced power conversion efficiency of the cell was ascribed to the increase in both conductivity and work function (W_P) of PEDOT:PSS film. The increased conductivity reduced the series resistance (R_S) within the cell, and the higher W_P generated the larger built-in potential (V_{bi}) which resulted in the improvement of the open-circuit voltage. In addition, the decreased R_S and enlarged V_{bi} were beneficial for the efficient charge transport/collection, contributing to the enhancement of the fill factor. Our results indicated that the conductivity as well as the W_P of the hole transporting layer played an important role in the organic-Si Schottky solar cell. © *2013 AIP Publishing LLC*. [http://dx.doi.org/10.1063/1.4812988]

Crystalline Si solar cell has hold more than 80% photovoltaic (PV) market share due to their excellent properties, such as high efficiency, long-term stability, and abundant raw materials.[1] However, the significant Si PV industry growth has been limited, not only resulting from the expensive Si wafer but also from the high fabrication cost. It has been estimated that the Si cell fabrication has consumed as much as 30% of the total manufacturing cost due to the high-temperature steps as well as the required complicated equipments.[2,3] Therefore, hybrid organic-Si solar cell has been proposed which could exploit the advantages of the solution-based process of organic materials, making it possible to fabricate the efficient Si solar cells with the low cost and simple method. In the past few years, many organic molecules, such as ionic liquid (IL),[4] copper phthalocyanine (CuPc),[5] and 2,2′,7,7′-Tetrakis-(N,N-di-4-methoxyphenylamino)−9,9′-spirobifluorene (Spiro-OMeTAD),[6] poly(3-hexylthiophene) (P3HT),[7,8] and polyaniline (PAN),[9,10] have been used to form the hybrid organic-Si solar cells. Among these materials, due to the high transparency and conductivity, solution-processed poly(3,4-ethylenedioxythiophene):polystyrenesulfonate (PEDOT:PSS) has attracted wide interests in the study.[11–17] As for the planar Si/PEDOT:PSS hybrid structure, the power conversion efficiency (PCE) of ~11% has been demonstrated.[14] The effect of Si passivation has been investigated. Compared to the cell with hydrogen-terminated Si surface (H-Si), the one with oxygen-terminated Si surface (SiO_x-Si) exhibited a 530-fold increase in the PCE, from 0.02% to 10.6%.[18] However, there were few reports about the effect of PEDOT:PSS film on the cell performance.[19]

PEDOT:PSS in aqueous solution is deposited on a substrate and a post-annealing process is indispensable to remove the residue water in the as-fabricated film. Because of the hygroscopy of PEDOT:PSS, the presence of water in ambient gas can reduce the conductivity as well as work function (W_P) of PEDOT:PSS film.[20–22] In this work, in order to investigate the electrical properties of PEDOT:PSS on the Schottky Si/PEDOT:PSS cell, the PEDOT:PSS film was annealed either in air or in nitrogen, respectively. The results showed that due to the enhanced conductivity and W_P of PEDOT:PSS film, the PCE of the cell increased from 6.40% in air to 9.30% in nitrogen. The mechanism had been discussed in detail by current-voltage, capacitance-voltage, external quantum efficiency, and transient photovoltage measurements.

Fig. 1 showed the schematic of the Schottky Si/PEDOT:PSS cell. N-type single-crystal Si (100) with a resistivity of 5~7 Ω cm and a thickness of 470 μm was methylated by a two-step chlorination/alkylation process.[23] After Si methylation, high conductive PEDOT:PSS (CLEVIOS PH 1000) mixed with 5 wt. % dimethyl sulfoxide (DMSO) and 0.1 wt. % Triton X-100 (from Aldrich) was spin-coated on the Si substrate and annealed at 140 °C for 20 min in air and nitrogen atmosphere, respectively. Silver grid electrodes with a 10×8 mm^2 area were deposited onto the organic layer for the efficient hole collection by vacuum thermal

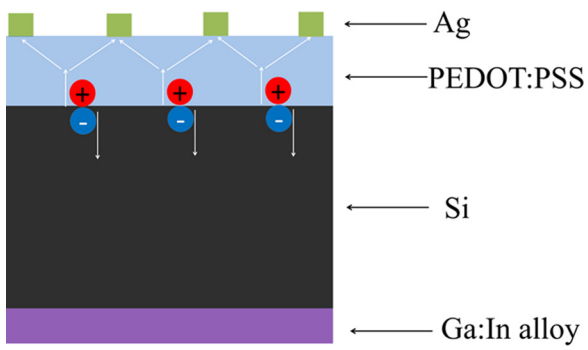

FIG. 1. Schematic of the Schottky Si/PEDOT:PSS cell. The ratio of the different layers is not in real scale.

[a)]Author to whom correspondence should be addressed. Electronic mail: bqsun@suda.edu.cn. Tel.: (86)-512-65880820. Fax: (86)-512-65882846.

 © 2013 AIP Publishing LLC

Downloaded 17 Sep 2013 to 147.26.11.80. This article is copyrighted as indicated in the abstract. Reuse of AIP content is subject to the terms at: http://apl.aip.org/about/rights_and_permissions

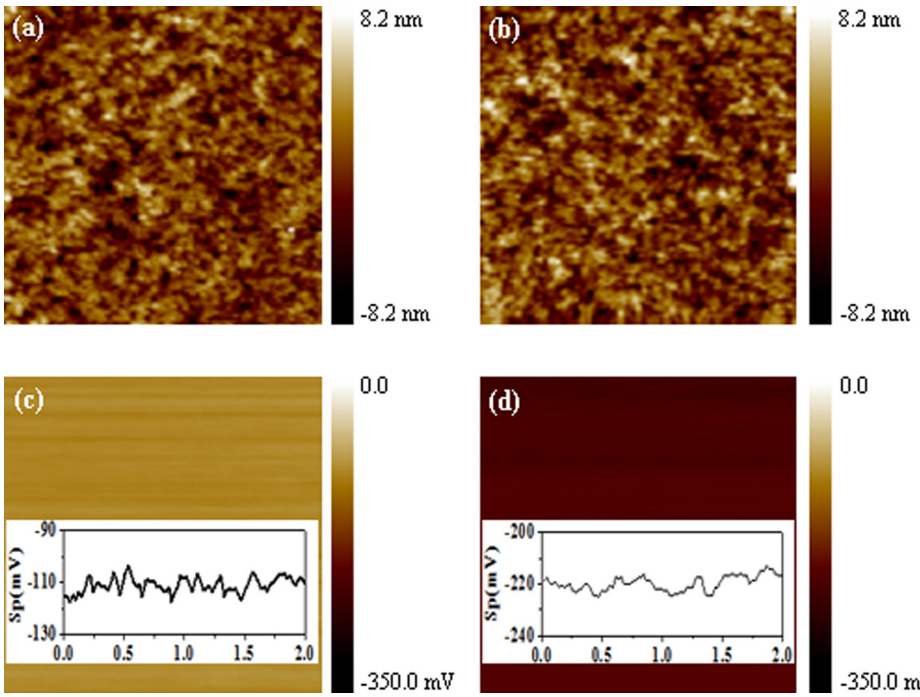

FIG. 2. AFM and SKPM images ($2 \times 2\,\mu$m) of PEDOT:PSS films annealed in different atmospheres. Topography of film annealed in (a) air and (b) nitrogen. SKPM image of film annealed in (c) air and (d) nitrogen. The insets in (c) and (d) were the line sections over the corresponding films.

evaporation. Finally, the back contact was obtained by rubbing a thin layer of In:Ga eutectic onto the rear side of the Si substrates.

In different atmospheres, the thicknesses of PEDOT:PSS films were close to 100 nm. However, the electrical properties were different. The conductivity of the film increased from 539 S/cm in air to 659 S/cm in nitrogen. As shown in Fig. 2, although the morphologies of PEDOT:PSS films were similar, the surface potential (V_{CPD}) of the film in nitrogen was 0.11 V lower than that of the film in air by means of the scanning Kelvin probe microscope (SKPM) method which meant that the W_p of the film in nitrogen was 0.11 eV higher via a equation of $W_P = \Phi_{tip} - eV_{CPD}$, where e is the elementary charge and the Φ_{tip} is the work function of the conductive tip.

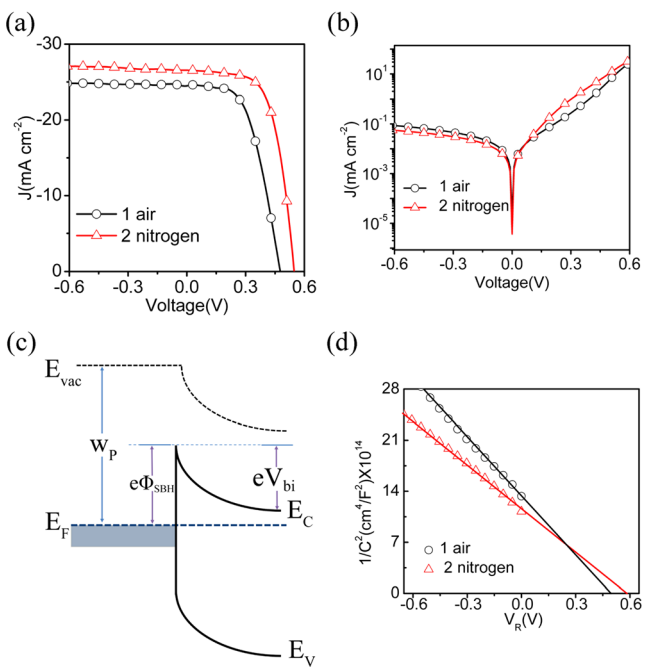

FIG. 3. J–V characters of the Schottky Si/PEDOT:PSS cells with PEDOT:PSS film annealed in different atmospheres (a) under AM 1.5G irradiation at 100 mW cm^{-2} and (b) in dark. (c) Band energy diagram of the PEDOT:PSS/Si interface. (d) Room-temperature inverse square of the capacitance ($1/C^2$) versus reverse bias (V_R) plots for the corresponding devices.

Fig. 3(a) showed the current density-voltage (J-V) characteristics of the Schottky Si/PEDOT:PSS cell with PEDOT:PSS films annealed in different atmospheres under air mass 1.5 global (AM 1.5 G) irradiation of 100 mW cm^{-2}. The electric output characteristics of the cells were summarized in Table I. Comparing with the cell (Device 1) based on PEDOT:PSS film formed in air, the short-circuit current density (J_{sc}), the open-circuit voltage (V_{oc}) and the fill factor (FF) of the cell (Device 2) based on the film formed in nitrogen all increased from 24.53 mA cm^{-2} to 26.36 mA cm^{-2}, 0.47 V to 0.54 V, and 0.555 to 0.655, respectively. The increased V_{OC} and FF boosted the PCE from 6.40% to 9.33%.

As shown in Fig. 1, due to the silver grid electrodes used, there was nearly 90% area without contacting the metal electrode, and the high conductivity of PEDOT:PSS was essential to allow the efficient charge collection. As a result, the dramatic improvement in the efficiency of Device 2 was partially contributed to the increased film conductivity as well as the associated reduction of Ohmic losses. The series resistance (R_s) was defined by the slope of the J–V curve at $J = 0$.[24] The R_s values of Device 1 and Device 2 were 6.67 and 3.53 Ω cm^2, respectively. Since lower R_s was beneficial

TABLE I. Electronic output characteristics of the Schottky Si/PEDOT:PSS cells with PEDOT:PSS films annealed in different atmospheres.

Annealing Atmosphere	J_{sc} (mAcm^{-2})	V_{oc} (V)	FF	PCE (%)	R_S (Ω cm^2)
Air (device 1)	24.53	0.470	0.555	6.40	6.67
N_2 (device 2)	26.36	0.540	0.655	9.33	3.53

Downloaded 17 Sep 2013 to 147.26.11.80. This article is copyrighted as indicated in the abstract. Reuse of AIP content is subject to the terms at: http://apl.aip.org/about/rights_and_permissions

for the charge transport and collection, the J_{sc} and FF of the device 2 were improved. The enhancement in V_{OC} was ascribed to the higher W_p of PEDOT:PSS film. Fig. 3(c) showed the band energy diagram at PEDOT:PSS/Si interface. Because the voltage of the device was linearly with the built-in potential (V_{bi}), and the V_{bi} was related to the Schottky barrier height (Φ_{SBH}) via the expression of $\Phi_{SBH} = V_{bi} + e^{-1}\,kT\,\ln(N_C/N_D)$,[25] where N_C is the effective density of states in the conduction band and N_D is the doping level of the semiconductor. According to an ideal Schottky-Mott model, the Schottky barrier height at the PEDOT:PSS/n-Si interface was proportional to the difference between the W_p and the electron affinity of Si (χ_{Si}) for an ideal interface state by a equation of $e\Phi_{SBH} = W_p - \chi_{Si}$. As methylation could successfully passivate Si surface,[8,26,27] there should be no difference for N_C and N_D in different post-annealing condition. The higher W_P of PEDOT:PSS film generated the larger Φ_{SBH} and V_{bi}, leading to the enhancement of V_{OC}. In addition, the increased V_{bi} allowed efficient charge transfer/collection, also contributing to the improvement of the FF.

By analyzing the dark J−V data of the devices, as shown in Fig. 3(b), we calculated the Φ_{SBH} for the Device 1 and Device 2 were 0.72 V and 0.81 V, respectively, with the help of the thermionic emission model of $J = J_S\left(\exp\left(\frac{e}{nkT}V\right) - 1\right)$ and $J_s = A^*AT^2\exp\left(-\frac{\Phi_{SBH}}{kT}\right)$,[28] where A is the contact area, A* is the effective Richardson constant ($\approx$252 $Acm^{-2}K^{-2}$ for n-type silicon), T is the absolute temperature (298 K), k is the Boltzmann constant, n is the diode ideality factor, J_S is the reversed saturation current in the diodes. The magnitude of V_{bi} can also be extracted from the plots of the capacitance versus bias voltage (C–V) characteristics. Within the Schottky-Mott relationship, the diodes of $1/C^2$ scales were linear with the reverse bias (V_R) and the extrapolation to the abscissa could yield V_{bi}. As shown in Fig. 3(d), it was observed that V_{bi} values of the Device 1 and Device 2 were 0.49 V and 0.58 V, respectively. Here, the 0.1 V enhancement in V_{bi}, which approximated to the 0.09 V increase in Φ_{SBH}, was consistent with 0.11 eV difference in W_P between the films used in devices.

External quantum efficiency (EQE) measured the percentage of the incident photons which eventually resulted in the free charges collected by the electrodes. Apart from the light absorption, the magnitude of EQE was highly affected by the electrical characteristics of the devices, such as the resistance of the electrodes, charge transfer, and collection efficiencies. As shown in Fig. 4(a), the EQE spectra of devices were similar and coincided with the Si absorption spectrum. However, the EQE magnitude of the Device 2 showed an absorption-wide-band improvement. Thereafter, we ascribed the improvement to the electrical effects which caused by the increased conductivity and W_P of PEDOT:PSS film. The increased conductivity reduced the Rs, and the higher W_P increased V_{bi}, both of which increased the electrical characteristics of the device and allowed the more efficient charge collection.

To further confirm the effect of the increased conductivity as well as the higher W_p of PEDOT:PSS film, we employed the transient photovoltage measurement to explore the charge recombination kinetics in the Schottky Si/PEDOT:PSS cell at the open circuit condition.[29–31] The detailed processes and typical curves of the transient photovoltage and photocurrent measurements were illustrated in Fig. S1 (see Ref. 32). Since the photogenerated electron-hole pairs were assumed to be independent of an applied bias and the recombination at the short circuit was small. The carrier concentration, N, which corresponded to the value of the stored charge for each open circuit voltage and was also proportional to the trap state density in the cell, could be obtained by integrating the capacitance over voltage by an equation of $N = \frac{1}{Aed}\int_0^{Voc} CdV$, where d is the film thickness. The smaller value of N illustrated that more photo-generated charges had been separated and collected by the electrode, leading to less carrier recombination. As shown in Fig. 4(b), due to the increased conductivity which reduced the R_S within the cell and higher W_P generating larger V_{bi}, we observed that the N value of the Device 2 was $2.46 \times 10^{13}\,cm^{-3}$, lower than that of Device 1 ($2.75 \times 10^{13}\,cm^{-3}$). Here, the lower N value of Device 2 was consistent with its higher FF and J_{sc}.

In summary, we found that both the conductivity and work function of PEDOT:PSS played an important role on the performance of the Schottky Si/PEDOT:PSS cells. The results addressed the physics governing electrical transport across the PEDOT:PSS/n-Si interface and showed the conductivity as well as W_P of PEDOT:PSS film was another key to achieve the high efficiency of hybrid Si/PEDOT:PSS solar cell. The increased conductivity could reduce the Rs of the cell and the higher W_P could create the larger V_{bi} which improved the V_{OC}. The enlarged V_{bi} as well as the reduced Rs allowed the efficient charge transfer/collection, contributing to the enhancement of the FF. Such understanding was critical to further improvement of similar organic-Si Schottky solar cells.

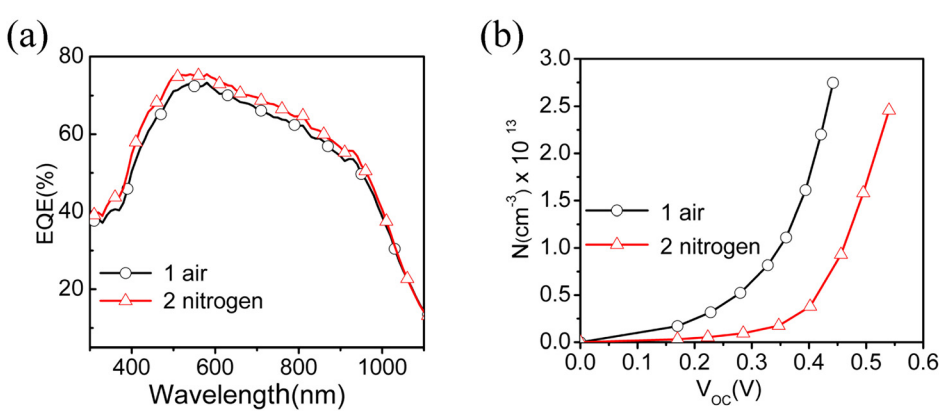

FIG. 4. (a) EQE spectra (b) Carrier concentration (N) versus V_{OC} of the Schottky Si/PEDOT:PSS cells with PEDOT:PSS films annealed in different atmospheres.

Downloaded 17 Sep 2013 to 147.26.11.80. This article is copyrighted as indicated in the abstract. Reuse of AIP content is subject to the terms at: http://apl.aip.org/about/rights_and_permissions

This work was supported by the National Basic Research Program of China (973 Program) (Grant No. 2012CB932402), and the National Natural Science Foundation of China (60976050, 61176057, 61211130358, 91123005). X.S. would like to thank Innovative Graduate Education Program of Jiangsu (No. CXZZ11_0098).

[1]R. F. Service, Science **319**, 718 (2008).
[2]V. M. Fthenakis and H. C. Kim, Sol. Energy **85**, 1609 (2011).
[3]R. G. Little and M. J. Nowlan, Prog. Photovoltaics **5**, 309 (1997).
[4]X. Shen, B. Sun, F. Yan, J. Zhao, F. Zhang, S. Wang, X. Zhu, and S. Lee, ACS Nano **4**, 5869 (2010).
[5]I. A. Levitsky, W. B. Euler, N. Tokranova, B. Xu, and J. Castracane, Appl. Phys. Lett. **85**, 6245 (2004).
[6]X. Shen, B. Sun, D. Liu, and S. Lee, J. Am. Chem. Soc. **133**, 19408 (2011).
[7]F. Zhang, X. Han, S. Lee, and B. Sun, J. Mater. Chem. **22**, 5362 (2012).
[8]F. Zhang, B. Sun, T. Song, X. Zhu, and S. Lee, Chem. Mater. **23**, 2084 (2011).
[9]W. N. Wang and E. A. Schiff, Appl. Phys. Lett. **91**, 133504 (2007).
[10]W. Wang, E. Schiff, and Q. Wang, J. Non-Cryst. Solids **354**, 2862 (2008).
[11]T. G. Chen, B. Y. Huang, E. C. Chen, P. Yu, and H. F.Meng, Appl. Phys. Lett. **101**, 033301 (2012).
[12]S. Jeong, E. C. Garnett, S. Wang, Z. Yu, S. Fan, M. L. Brongersma, M. D. McGehee, and Y. Cui, Nano Lett. **12**, 2971 (2012).
[13]T. G. Chen, B. Y. Huang, H. W. Liu, Y. Y. Huang, H. T. Pan, H. F. Meng, and P. Yu, ACS Appl. Mater. Interfaces **4**, 6857 (2012).
[14]Q. Liu, M. Ono, Z. Tang, R. Ishikawa, K. Ueno, and H. Shirai, Appl. Phys. Lett. **100**, 183901 (2012).
[15]B. Ozdemir, M. Kulakci, R. Turan, and H. E. Unalan, Appl. Phys. Lett. **99**, 113510 (2011).
[16]W. Lu, C. Wang, W. Yue, and L. Chen, Nanoscale **3**, 3631 (2011).
[17]S.-C. Shiu, J.-J. Chao, S.-C. Hung, C.-L. Yeh, and C.-F. Lin, Chem. Mater. **22**, 3108 (2010).
[18]L. N. He, C. Y. Jiang, H. Wang, D. Lai, and Rusli, Appl. Phys. Lett. **100**, 073503 (2012).
[19]M. Pietsch, M. Bashouti, and S. Christiansen, J. Phys. Chem. C **117**, 9049 (2013).
[20]J. S. Huang, P. F. Miller, J. S. Wilson, A. J. de Mello, J. C. de Mello, and D. D. C. Bradley, Adv. Funct. Mater. **15**, 290 (2005).
[21]J. Huang, P. F. Miller, J. C. de Mello, A. J. de Mello, and D. D. C. Bradley, Synth. Met. **139**, 569 (2003).
[22]N. Koch, A. Vollmer, and A. Elschner, Appl. Phys. Lett. **90**, 043512 (2007).
[23]A. Bansal, X. Li, I. Lauermann, N. S. Lewis, S. I. Yi, and W. H. Weinberg, J. Am. Chem. Soc. **118**, 7225 (1996).
[24]D. Pysch, A. Mette, and S. W. Glunz, Sol. Energy Mater. Sol. Cells **91**, 1698 (2007).
[25]S. M. Sze, *Physics of Semiconductor Devices* (John Wiley and Sons, New York, 1981).
[26]A. Bansal and N. S. Lewis, J. Phys. Chem. B **102**, 1067 (1998).
[27]M. Bashouti, T. Stelzner, A. Berger, S. Christiansen, and H. Haick, J. Phys. Chem. C **113**, 14823 (2009).
[28]X. Li, H. Zhu, K. Wang, A. Cao, J. Wei, C. Li, Y. Jia, Z. Li, X. Li, and D. Wu, Adv. Mater. **22**, 2743 (2010).
[29]C. G. Shuttle, B. O'Regan, A. M. Ballantyne, J. Nelson, D. D. C. Bradley, J. de Mello, and J. R. Durrant, Appl. Phys. Lett. **92**, 093311 (2008).
[30]A. H. Ip, S. M. Thon, S. Hoogland, O. Voznyy, D. Zhitomirsky, R. Debnath, L. Levina, L. R. Rollny, G. H. Carey, A. Fischer, K. W. Kemp, I. J. Kramer, Z. Ning, A. J. Labelle, K. W. Chou, A. Amassian, and E. H. Sargent, Nat Nanotechnol. **7**, 577 (2012).
[31]Z. Li, F. Gao, N. C. Greenham, and C. R. McNeill, Adv. Funct. Mater. **21**, 1419 (2011).
[32]See supplementary material at http://dx.doi.org/10.1063/1.4812988 for the detailed processes and typical curves of the transient photovoltage and photocurrent measurements.

Downloaded 17 Sep 2013 to 147.26.11.80. This article is copyrighted as indicated in the abstract. Reuse of AIP content is subject to the terms at: http://apl.aip.org/about/rights_and_permissions